

Open Research Online

The Open University's repository of research publications and other research outputs

Silence on Shangri-La: attenuation of Huygens acoustic signals suggests surface volatiles

Journal Item

How to cite:

Lorenz, Ralph D.; Leese, Mark R.; Hathi, Brijen; Zarnecki, John C.; Hagermann, Axel; Rosenberg, Phil; Towner, Martin C.; Garry, James and Svedhem, Håkan (2014). Silence on Shangri-La: attenuation of Huygens acoustic signals suggests surface volatiles. *Planetary And Space Science*, 90 pp. 72–80.

For guidance on citations see [FAQs](#).

© 2013 Elsevier Ltd.

Version: Accepted Manuscript

Link(s) to article on publisher's website:
<http://dx.doi.org/doi:10.1016/j.pss.2013.11.003>

Copyright and Moral Rights for the articles on this site are retained by the individual authors and/or other copyright owners. For more information on Open Research Online's data [policy](#) on reuse of materials please consult the policies page.

oro.open.ac.uk



Silence on Shangri-La: Attenuation of Huygens acoustic signals suggests surface volatiles

Ralph D. Lorenz^{a,*}, Mark R. Leese^b, Brijen Hathi^b, John C. Zarnecki^b, Axel Hagermann^b, Phil Rosenberg^c, Martin C. Towner^d, James Garry^e, Håkan Svedhem^f

^a Johns Hopkins University, Applied Physics Laboratory, Laurel, MD 20723, USA

^b The Open University, Milton Keynes, UK

^c University of Leeds, Leeds, UK

^d Department of Applied Geology, Curtin University, Perth, Australia

^e Red Core Consulting, Burnaby, British Columbia, Canada

^f European Space Agency, ESTEC, Noordwijk, The Netherlands

ARTICLE INFO

Article history:

Received 25 July 2013

Received in revised form

9 November 2013

Accepted 11 November 2013

Keywords:

Instrumentation

Acoustics

Planetary atmospheres

Organic chemistry

Attenuation

Huygens probe

ABSTRACT

Objective: Characterize and understand acoustic instrument performance on the surface of Titan.

Methods: The Huygens probe measured the speed of sound in Titan's atmosphere with a 1 MHz pulse time-of-flight transducer pair near the bottom of the vehicle. We examine the fraction of pulses correctly received as a function of time.

Results: This system returned good data from about 11 km altitude, where the atmosphere became thick enough to effectively transmit the sound, down to the surface just before landing; these data have been analyzed previously. After an initial transient at landing, the instrument operated nominally for about 10 min, recording pulses much as during descent. The fraction of pulses detected then declined and the transmitted sound ceased to be detected altogether, despite no indication of instrument or probe configuration changes.

Conclusions: The most likely explanation appears to be absorption of the signal by polyatomic gases with relaxation losses at the instrument frequency, such as ethane, acetylene and carbon dioxide. These vapors, detected independently by the GCMS instrument, were evolved from the surface material by the warmth leaking from the probe, and confirm the nature of the surface materials as 'damp' with a cocktail of volatile compounds. Some suggestions for future missions are considered.

Practice implications: None.

© 2013 Elsevier Ltd. All rights reserved.

1. Introduction

Titan is unique among the satellites of the solar system in that it has an atmosphere. This makes it of particular interest to acousticians (e.g. Leighton and White, 2004; Leighton and Petculescu, 2009) since the propagation of sound is of interest in its own right, both for education/outreach as well as for science, and for serving as a means to study winds and transient phenomena such as precipitation, wave breaking, thunder, volcanic eruptions and bolide entry. Titan's thick atmosphere is favorable for the generation and receipt of soundwaves by transducers, and the low temperatures make the attenuation by the principal constituent gases nitrogen and methane relatively low (e.g. Petculescu and Lueptow, 2007; Hanford and Long, 2009). However, photochemistry in the upper atmosphere generates a wide range of

complex organic molecules (some of which make up Titan's hydrocarbon seas, and perhaps also its fields of giant sand dunes). These molecules, present only as traces in the atmosphere but in potentially large accumulations on the surface, can be strongly absorbing to ultrasound.

Although the Cassini spacecraft in Saturn orbit continues to make remarkable findings at Titan and motivates future in-situ exploration by landers, balloons or other platforms, the only available in-situ environmental data from Titan's surface is that from the Huygens probe, from which data were received for 72 min after its landing at the western margins of the Shangri-La dunefields near Titan's equator. It is therefore important to examine these data, hard-won from Titan's cryogenic environment, for whatever insights they may offer – even when the data were not necessarily acquired through the expected operation of the relevant instrumentation. A number of proposed future investigations have considered ultrasonic anemometers (e.g. the dune lander on the 2007 Flagship mission study 'Titan Explorer',

* Corresponding author. Tel.: +1 443 778 2903; fax: +1 443 778 8939.

E-mail address: ralph.lorenz@jhuapl.edu (R.D. Lorenz).

Leary et al., 2007, and the Titan Mare Explorer (TiME) capsule proposed to NASA's Discovery program to float on the sea Ligeia Mare in 2023, Stofan et al., 2013; Lorenz et al., 2012), depth sounders (e.g. in the lake lander study in the Titan Saturn System Mission TSSM, ESA, 2009, and the Decadal Survey lake lander study, JPL, 2010, and TiME, Lorenz et al., 2012), and passive microphones (Titan Explorer and TSSM). Of these studies, the Titan Mare Explorer (TiME) was the most advanced, with detailed study of sonar operation (e.g. Arvelo and Lorenz, 2013) and cryogenic testing of prototype acoustic transducers (Lorenz et al., 2012). Given this recurrent interest we therefore reexamine here the surface operation of the Huygens acoustic instrumentation, whose results were not interpreted previously.

The Huygens probe to Titan carried three acoustic instruments. A passive microphone, part of the Huygens Atmospheric Structure Instrument (HASI) was intended to search for thunder, but detected only aeroacoustic noise during descent. The Surface Science Package (SSP) carried a down-pointing sonar, the Acoustic Properties Instrument – Sounder (API-S) which detected an echo from the surface during the last seconds of parachute descent (Zarnecki et al., 2005; Towner et al., 2006), and a speed-of-sound sensor (Acoustic Properties Instrument – Velocity, or API-V). It is this latter instrument that forms the topic of the present paper.

2. Instrumentation

When the Huygens probe was conceived, a prevailing model for Titan's surface was of a global ocean and, while post-landing survival was not guaranteed, the possibility of making brief measurements on the surface was recognized. The probe specification demanded that it float, and that the battery energy and communications budgets permit at least 3 min of surface operations. One quick measurement that was included as a diagnostic of the methane:ethane ratio in the ocean was a speed of sound measurement, implemented within the Surface Science Package (SSP) on the probe (Zarnecki et al., 1997, 2002). This measurement (as others such as dielectric constant and refractive index in the SSP) required sensors to be immersed in the ocean, and so these were mounted near the apex of the probe (Fig. 1).

The speed of sound measurement on Huygens was very simple in concept: a pair of transducers are separated by a known distance (12.89 cm), and the propagation time of a pulse of ultrasound (1 MHz)

across that distance is measured by starting a clock on emission at one transducer and stopping it on receipt at the other. In practice (e.g. Rosenberg, 2007; Hagermann et al., 2007) the simple design using a threshold detector on the receive circuit (and, possibly, the fact that the receiver is at the edge of the near field of the transmitter) led to some subtleties in performance.

The principal objective of the measurement was to diagnose liquid composition, and to provide a sound speed to permit the echo delay time from a small acoustic depth-sounder to be interpreted as an ocean depth. During development it was realized that meaningful data might also be obtained during descent (e.g. Lorenz, 1994; Garry, 1996; Zarnecki et al., 1997; Svedhem et al., 2004).

The instrument consisted of two sensor heads (API-V1 and API-V2) each containing a piezoelectric element (PXE-5) able to act as both a transmitter and a receiver; the elements (with an exposed diameter of about 14 mm) were mounted in small alloy housings and had a thin layer of syntactic foam added to improve coupling into the atmosphere. The sensor heads were mounted opposite and facing each other across the SSP cavity (Fig. 2) allowing atmospheric gases to flow past them. The sensors were mounted at the opening of the cavity, but behind an electromagnetic shield (Fig. 3) designed to prevent damage to the instrumentation from any lightning or electrostatic discharge.

To make a measurement, a 1-MHz wavetrain of nominally 10 μ s duration (i.e. 10 cycles) was transmitted between the sensors and the time of flight of this sound wave was measured. The timing clock had a frequency of 4 MHz giving a time resolution for the measurement of 0.25 μ s. This process was repeated twice per second (once in each direction, the propagation time from API-V1 to API-V2 being designated T1, and vice-versa as T2.) potentially providing a vertical resolution during the descent through Titan's atmosphere of just a few meters.

Experimentation with flight spare sensors revealed that it takes a time $t_0 = 3.71 \mu$ s for the sound waves to propagate out of the transmitting sensor and into the receiving sensor, assuming zero free-space separation. It is clear that this value of t_0 is determined by the capacitance of the piezoelectric crystals as well as the thickness of, and speed of sound within, the crystals and their impedance matching coatings.

Experimentation with flight spare sensors also revealed that the envelope of the received signal is more bell shaped than the

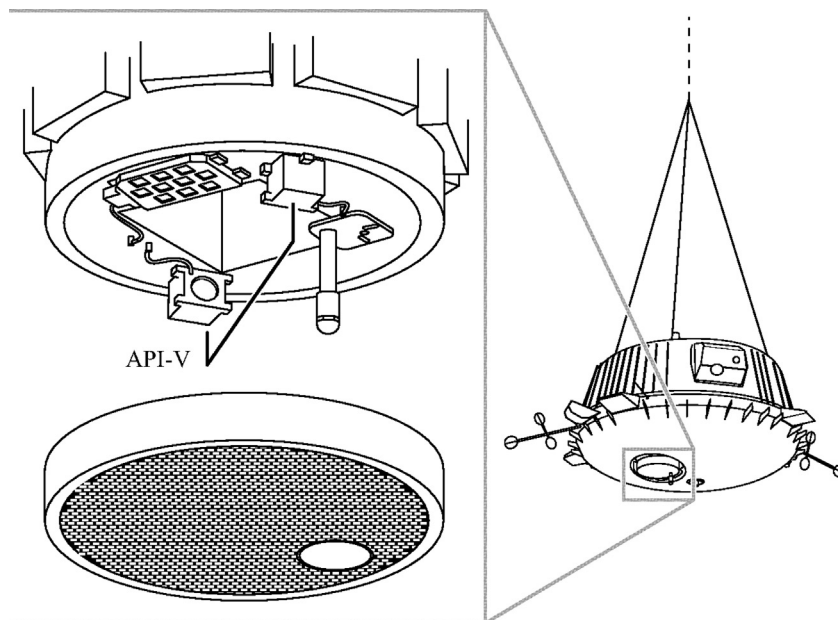


Fig. 1. Location of the SSP API-V sensors on the underside of the Huygens probe, with the anti-static screen shown displaced downwards for clarity.

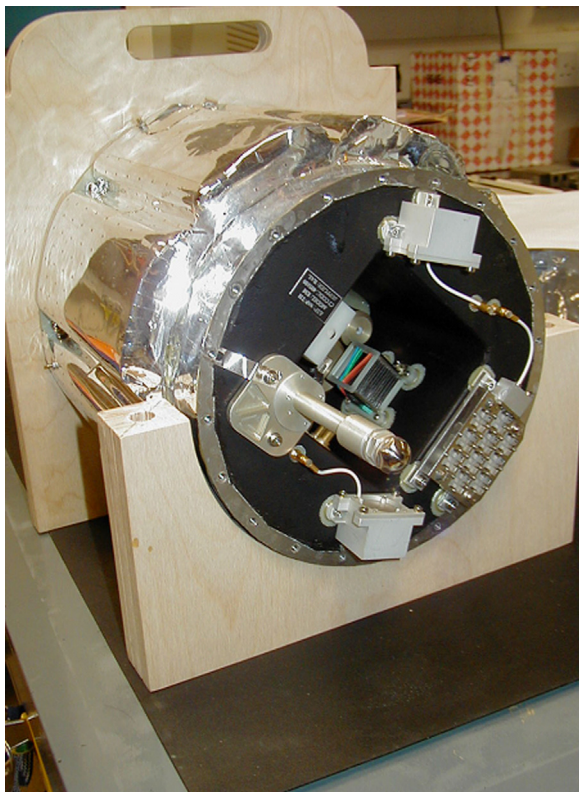


Fig. 2. View of the SSP 'Top Hat' structure with the grill removed. The metallic boxes at top and bottom are the API-V speed of sound transducer housings (the circular transducer surface is just visible on the right one). The penetrometer is visible at left (note also the grounding strap) and the acoustic sounder at lower right.

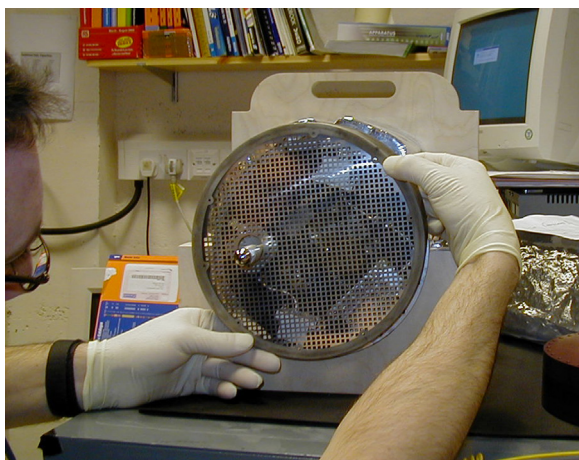


Fig. 3. The metal grill shown in position on the front of the SSP Top Hat. Most photographs of the probe show the instrumentation with the grill removed, but it is important in understanding the possible influences on the acoustic instrumentation.

transmitted signal. This effect, due to the resonant response of the transducer with finite Q , means that early peaks in the signal train may not have large enough amplitude to be detected. Each peak missed in this way causes API-V to overestimate the time of flight by $1 \mu\text{s}$. Before encounter it was expected that, as the probe descended and the density of the atmosphere increased, the received signal would become stronger and fewer peaks would be missed in this way. This would manifest itself in the flight data in the form of discontinuities separated by $1 \mu\text{s}$ in a plot of time of flight vs altitude.

Given the trigger voltage threshold on the flight sensor of 69.9 mV, operation was expected to require a transmission coefficient of at least $\sim 0.315 \times 10^{-3}$ which, using room temperature data for the sensor materials, corresponds to a required impedance of the sampled gas of at least ~ 629 Rayl (see, e.g. Rosenberg, 2007). Examining the predicted engineering model for Titan's atmosphere, it should have been expected that the sensor would begin to operate at around 10–12 km altitude. Acoustic absorption by gases in the free atmosphere across this short transmission path was expected to be minimal (e.g. Svedhem et al., 2004, and more recent calculations by Petculescu and Achi (2012)).

3. Data

The data analyzed here are the propagation times measured by the API-V instrument during the descent, as calibrated and archived on the NASA Planetary Data System (PDS). The data are in the Huygens SSP archive maintained on the PDS Atmospheres Node at New Mexico State University (presently, http://atmos.pds.nasa.gov/data_and_services/atmospheres_data/Huygens/SSP.html) and are mirrored on the European Space Agency Planetary Science Archive (PSA). The data (filename SSP_APIV_123456_0_R_ATMOS.TAB) comprise a tabulation of sample times relative to the spacecraft reference T0 (the firing of the parachute mortar at the end of the hypersonic entry into the atmosphere), an instrument mode flag and record number, and the two times for propagation of the sound pulse in each direction, expressed in the raw digital counter number, and as a time in milliseconds. Documentation of the data is in the PDS data label file SSP_APIV_123456_0_R_ATMOS.LBL and the calibration file SSP_CALASC.

The latter file notes that the distance between the two transducer faces is 0.1289 m, and that the digital counter number refers to a 4 MHz clock. As discussed in the text above and in Hagermann et al. (2007), there is a $\sim 3.7 \mu\text{s}$ offset to account for the propagation out of and into the transducers.

Fig. 4 shows the recorded API-V dataset taken during Huygens descent. Although API-V was switched on only 600 s after initial parachute deployment, the upper atmosphere was too tenuous for sufficient atmosphere–sensor coupling and the first successful measurement occurred once the probe descended into sufficiently dense air, at an altitude of just above 11 km (the temperature and pressure at this point were recorded by the probe at ~ 83 K and

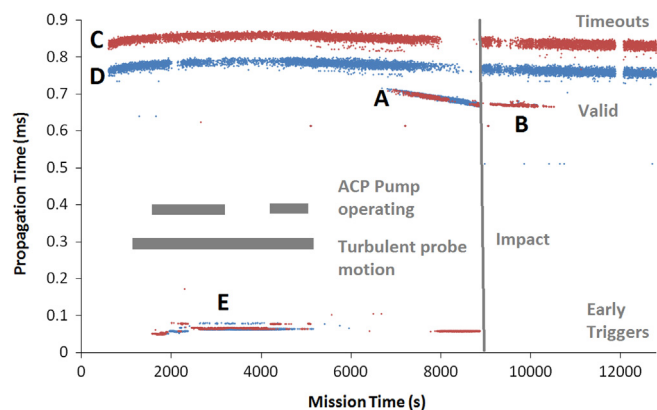


Fig. 4. The API-V data against mission time. The 'good' propagation times in milliseconds (A) measured during the lower part of descent have been analyzed in detail by Hagermann et al. (2007). Surface measurements (B) are discussed in the present paper. For most of the descent, the receive pulse threshold was not crossed and the counter timed out, forming two clouds of points (C, D) – the timeout was different for the two propagation directions (red points C refer to T1, blue points to times T2). A spurious set of early triggers (E) are present and are discussed in the text and may be related to noise from the Aerosol Collector Pyrolyzer (ACP) pump.

830 mbar). It can be seen that the propagation time decreases as descent proceeds left to right (speed of sound decreases with altitude, an effect caused mostly by the associated decrease in temperature). There is also a scatter in the retrieved sound speeds of approximately 3 ms^{-1} , much larger than the expected absolute accuracy of the sensors of 0.3 ms^{-1} based upon the accuracy of measuring the time of flight and the sensor separation. This spread of data has been studied by taking the difference between the measured time of flight and the value expected for pure nitrogen for all measurements taken below 6 km. A random number of peaks is seen during each measurement instead of simply missing fewer as the pressure increases. The effect is much reduced on the surface with a scatter of less than 1 ms^{-1} . Turbulent eddies passing between the sensors during descent might have caused a seemingly random change of the scattering properties of the gas, creating this effect. This means that each data point can be considered a lower limit on the speed of sound with a relative resolution better than 7.5 cm s^{-1} based on the $0.25 \mu\text{s}$ sampling rate; but the absolute speed of sound could be higher by integer multiples of $\sim 30 \text{ cm s}^{-1}$, based on the 1 MHz pulse frequency.

3.1. Descent timeouts and spurious early triggers

In order to obtain a high vertical resolution, e.g. to characterize the planetary boundary layer, measurements are made once every second. Although it was only expected that the acoustic impedance of the atmosphere would become large enough to reliably detect the transmitted pulse towards the end of descent (when the

atmosphere would be about 1000 times denser than at the start) measurements began at the beginning of descent. Failing to detect a strong enough pulse would result in the clock timing out, implying an unphysically large propagation time – these events are shown in the clouds C, D of points in Fig. 4.

A small variation in the actual value of the timeout clock timer is presumably related to parametric drift in the timer components: the SSP electronics temperatures (e.g. Leese et al., 2012) show a time history very similar to the envelope of the timeouts, with a small increase from the beginning until about 3000 s, and a slow decline thereafter. The expected timeouts were observed through time 1571 s, when T1 triggers early, and then more frequently through ~ 1844 s, when T2 also triggers early.

These early triggers (the cloud of points E in Fig. 4) are then seen, often in bursts, on both channels and in fact more often on T2, until at about 4700 s they cease and timeouts resume consistently.

It is tempting to associate these anomalous early triggers with the cause of noise seen on the sounder instrument which we know to be due to the operation of a high speed pump on the Aerosol Collector/Pyrolyzer instrument (see the pump current and speed history in housekeeping data archived at http://atmos.nmsu.edu/PDS/data/hpacp_0001/DATA/ACP_PUMP_V1_0.TAB). This fan operated at around 25,000 rpm from 1500 s until 3500 s, and 4650–5310 s. Thus the correspondence of the API-V triggers is far from complete and another explanation must be sought for at least some of the triggers. It seems likely that some kind of turbulence or aeroacoustic effect may have been responsible. Most curiously, when the instrument appears to be operating nominally in the

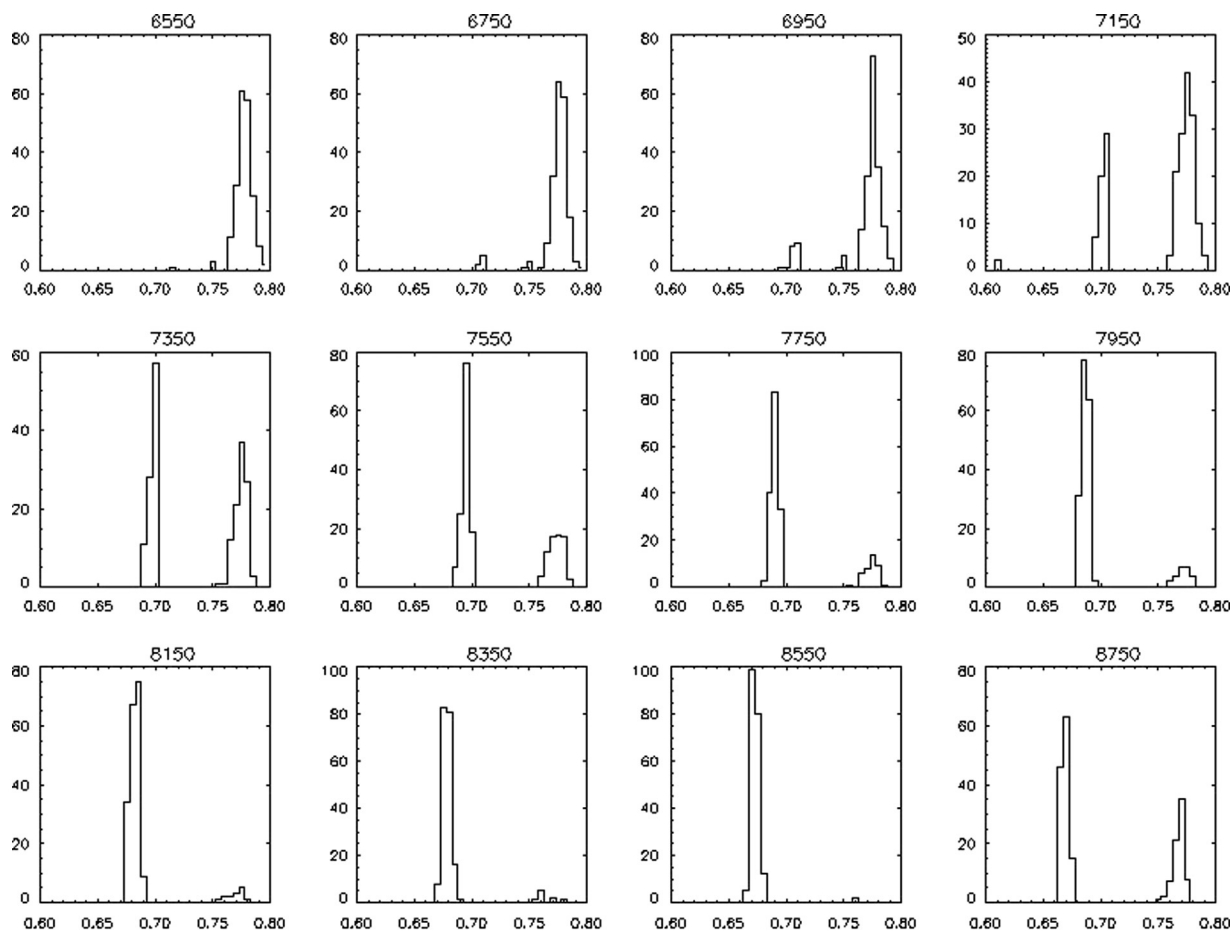


Fig. 5. Statistics of T2 propagation times (milliseconds) in 200 s blocks leading up to landing (dataset A in Fig. 4). The left peak corresponds to valid pulses, while the right peak are timeouts (C, D in Fig. 4). Initially (6650 s, about 14 km) there are no received pulses and only timeouts at ~ 0.78 ms are present. As the probe descends into denser air, propagated pulses begin to appear correctly at ~ 0.7 ms and progressively dominate, with almost no timeouts present after ~ 8000 s, until the last 1 km of descent. Why this should occur is not clear.

lower atmosphere (where the dense gas allows good coupling and thus a strong signal) T1 again begins to sporadically trigger early at 7767 s (at about 5 km altitude), then again at 7870 s, and with increasing frequency through ~8000 s where it triggers most of the time until landing at 8870 s.

Some support for an aerodynamic explanation derives from the fact that no early triggers occurred after landing. Furthermore, the motions of the probe were recorded by accelerometers and tilt sensors (e.g. Lorenz et al., 2007) which documented that the probe was buffeted significantly prior to 5500 s, but was fairly quiescent thereafter. Although ground tests showed that the fairly narrow sound beam between the transducers can be scattered by modest airflow (e.g. from a desk fan) which would lead to timeouts, turbulent airflow in the SSP cavity seems unlikely to be the cause of early triggers, since flow through the instrument is limited by a narrow vent tube, and the ESD grille (Fig. 3) would further suppress airflow fluctuations. Perhaps the most likely cause of early triggers is vibrations from structural flexing of the probe due to the turbulent motion in this period. The relative occurrence of early triggers and valid pulse propagation during the latter part of descent is shown in histogram form in Fig. 5.

3.2. Post-landing suppression of propagation

The post-impact record of timeouts and valid pulses is shown in histogram form in Fig. 6, and as a moving average 'success rate'

in Fig. 7. Initially the system does not detect valid pulses but after a short period begins to work nominally. Later, however, the success rate declines slowly to zero, without any obvious associated events on the probe.

The post-landing environment of the Huygens probe was very quiescent after the first ~6 s when there was some bouncing and skidding (Bettanini et al., 2008; Schroeder et al., 2012). The orientation of the probe changed very slightly, with a tilt of ~0.2° occurring over 72 min (Karkoschka et al., 2007). The camera observed no other changes, apart from a possible methane dewdrop forming on the camera baffle and falling through the field of view (Karkoschka and Tomasko, 2009) – this was observed on Image #897 which was acquired at T0+10, 423 s, i.e. 1553 s after landing. Additionally, material either inside or immediately adjacent to the heated inlet of the GCMS instrument progressively warmed up after landing (Lorenz et al., 2006) and evolved methane, and later ethane and some other compounds (Niemann et al., 2005, 2010). The thermal interactions of the warm – but well-insulated and therefore cold-skinned – probe with the surface environment are discussed in Lorenz (2006).

Since no major temperature changes occurred, and no major change in position, some changes in the material around or between the transducers seem to have been responsible for the drop in received signals. One hypothesis speculatively advanced in a thesis by Rosenberg (2007) was that liquid from the damp subsurface seeped into the cavity made by the probe and reduced the atmospheric coupling between the transducers by allowing

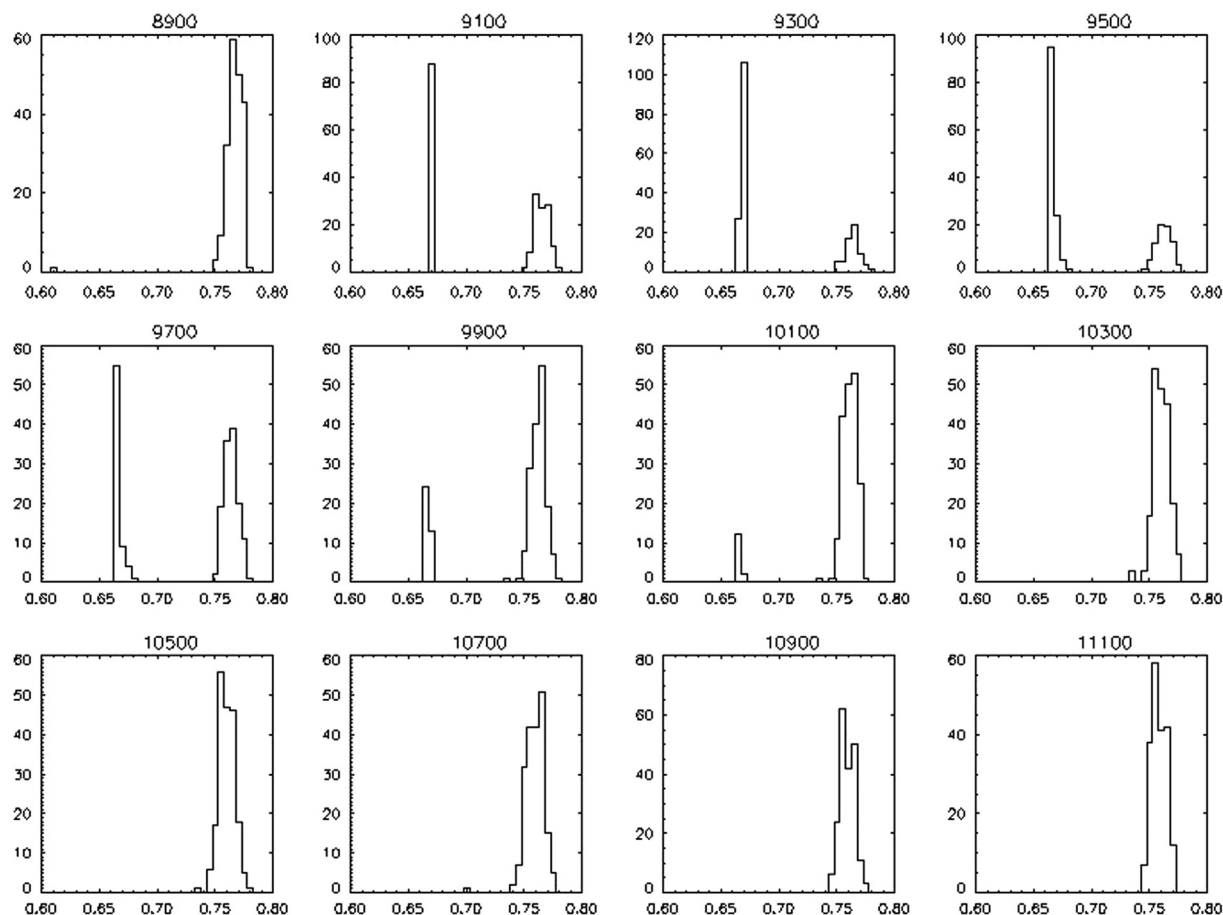


Fig. 6. Statistics of propagation times (x-axis, milliseconds) in 200 s blocks of data after landing (dataset B in Fig. 4). The right-hand peaks (> 0.72 ms) correspond to timeouts, the left hand peak to valid pulse receipt. Data start 30 s after the impact at 8870 s – it is known that the probe was still moving for a few seconds after contact. Initially (8900–9100 s) there are no clean pulses, perhaps as a result of material adhering to the transducers. Over 9100–9500 s a good strong signal builds up and the proportion of timeouts declines, but then increases again over 9500–10300 s, with no further clean pulses getting through thereafter. Notice also that while at 9100–9300 s the 'good' pulse histogram is sharp indicating clean triggers from a strong signal, the histogram for 9700 s and thereafter is broader and positively skewed, i.e. with a fraction of 'late' triggers. As discussed in Hagermann et al. (2007) this is a signature of a weak signal.

some of the pulse energy to propagate into the liquid and surface material. This scenario could be considered under the paradigm that the probe penetrated into the ground, decelerating over a distance of around 15 cm (e.g. Zarnecki et al., 2005). However, understanding of the probe post-impact motion has since improved (Schroeder et al., 2012), concluding that the probe bounced or skidded out of this impact depression. There is evidence that the probe was left sitting on the surface, rather than having penetrated into it (from the camera geometry, Karkoschka et al., 2007, and from the multipath interference pattern observed in the Huygens radio signal, Pérez-Ayúcar et al., 2006). Thus a liquid intrusion scenario seems unlikely.

On the other hand, the introduction of heavier gases into the SSP cavity between the transducers may have dramatically reduced the pulse strength. With small amounts of gas, the sound speed would not be significantly affected, yet the attenuation at 1 MHz could be substantially increased, as we note in the next section. It is seen in Fig. 4 that the post-impact propagation times decrease slowly, as would be expected from either warming, or a decrease in the relative molecular weight (due to an increasing methane concentration). However, even assuming the temperature evolution of the instrument (see later) to be representative of the acoustic cavity, the interpretation of the post-impact sound speed is not unique, since higher molecular weight gases may have partially offset the methane abundance.

4. Temperature environment and candidate gas evolution

If we hypothesize that the nondetection of pulses post-landing is due to the introduction of an attenuating gas into the SSP cavity, then we can use the descent data as a proxy calibration. Specifically, for the absorber to cause the loss of signal, it must introduce an attenuation equivalent to the difference in transmission between the unperturbed atmosphere at the surface and the atmosphere at the altitude where a similarly low pulse detection rate was encountered. Specifically, since the detection rate was near-zero at ~ 10 km altitude, the surface absorber must have attenuated the signal by a factor of $\sim (\rho_{10}c_{10}/\rho_0c_0)^2$ or $[(3.5 \times 184)/(5.4 \times 194)]^2 = 0.37$, roughly 1 np or 8.7 dB. Thus the localized atmosphere in the SSP cavity has an attenuation coefficient α of $8.7/0.12 \sim 70$ dB/m or ~ 8 np/m: it is probable that this aggregate attenuation is the result of the absorption by several different gas species together, each at a modest concentration.

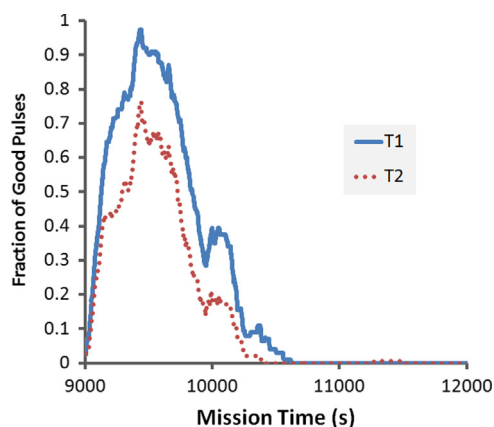


Fig. 7. 200-sample running mean of the fraction of good pulses (i.e. transit times in the valid range of 0.6–0.7 ms) in the two directions (T1, T2) just after landing. In fact the performance jumps rapidly upwards after landing (the 200-sample smoothing limits the gradient, but shows better the quantitative decline in performance after 9500 s).

Dain and Lueptow (2001) examine the attenuation in methane–air mixtures, showing that the attenuation ($\alpha\lambda$) at 600 kHz/bar is substantially influenced by molecular relaxation of methane, having $\alpha\lambda \sim 0.01$ for high methane concentrations at 297 K. For the wavelength of the Titan experiment with $c \sim 200$ m/s, $\lambda \sim 0.2$ mm and thus $\alpha \sim 50$ np/m for pure methane. The methane concentration was measured (Niemann et al., 2005) to be $\sim 5\%$ in the free atmosphere (where of course the pulses were transmitted successfully), but it could have risen slightly in the SSP cavity. Heavier gases which were essentially absent in the free atmosphere but which may have accumulated in the warming cavity seem a more likely candidate to provide the incremental attenuation. Ethane is a strong candidate (see later) but there are several others (see Figs. 8 and 9) and it will not be possible to discriminate their contributions since measurements at only one frequency were made.

Martinsson and Delsing (2002) give measurements of the attenuation of (pure) ethane at 600 kHz/bar (i.e. the condition of the 1 MHz measurement at 1.5 bar) of 30–40 np/m. The corresponding attenuation of Carbon monoxide was ~ 10 np/m. Holmes et al. (1964) obtain a similar value for ethane, and find propane to have an attenuation about a factor of 2 lower. All these data are at room temperature.

The quantitative interpretation of the Huygens measurement really requires low-temperature attenuation measurements which are not, as far as the authors are aware, available. The actual gas mixture that formed in the acoustic cavity on Huygens cannot in any case be uniquely determined: our only intent here is to show that methane, ethane and carbon dioxide (compounds known to be present on the Titan surface) and other organics (like ethylene and many others) can provide significant acoustic absorption at the frequencies discussed.

Niemann et al. (2005, 2010) show that the GCMS instrument detected several species after landing (see Fig. 10). Note that there is no expectation of an exact correspondence between the GCMS readings and the gas abundances in the SSP cavity for several reasons. First, the thermal histories of whatever material was jammed into the heated GCMS inlet or warmed around it, and that of the SSP cavity and the ground beneath, will have differed in details. Further, the diffusion of vapors warmed by the inlet into the gas sampling tubes would have introduced some delay into their detection, whereas the SSP cavity would be more

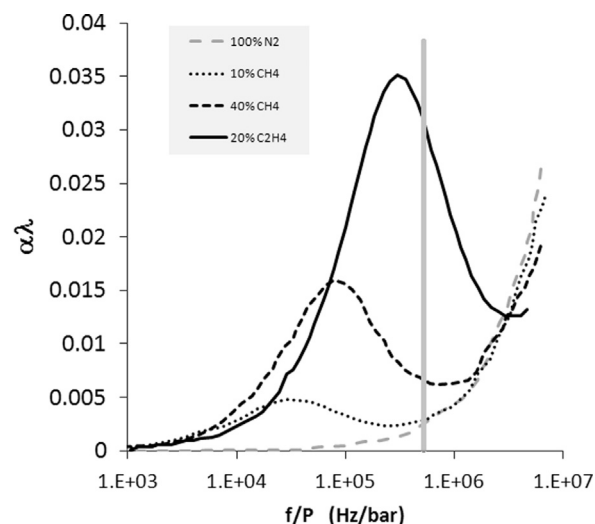


Fig. 8. Dimensionless attenuation of several gases mixed with nitrogen. The Huygens API-V measurement on the surface corresponds to $f/P = 6E5$ Hz/bar, rather close to where the ethylene absorption has a peak. Curves extracted from Petculescu et al. (2006) and Dain and Lueptow (2001); see also Ejakov et al. (2003).

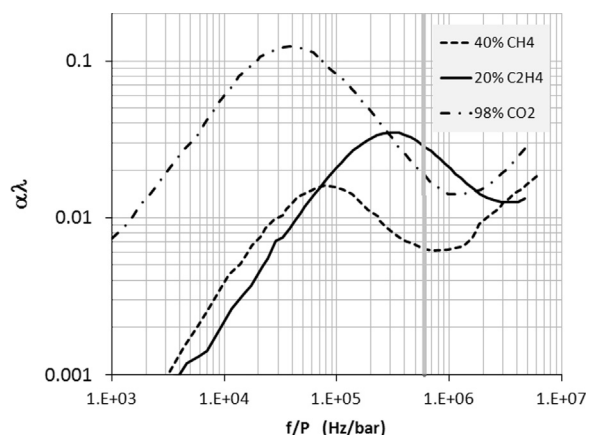


Fig. 9. Dimensionless attenuation for several gas mixtures. Note the very strong absorption by CO_2 , although this peaks at a frequency an order of magnitude lower than that for ethylene (C_2H_4). Curves extracted from Petculescu et al. (2006) and Dain and Luetpew (2001); see also Ejakov et al. (2003).

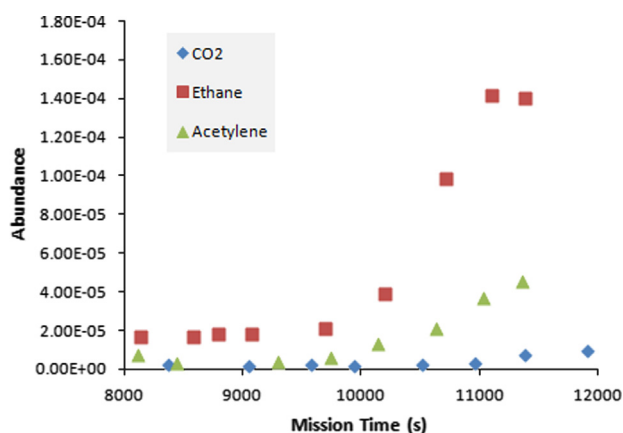


Fig. 10. The mixing ratio evolution of some acoustically-absorbing gases sampled by the Huygens GCMS (Niemann et al., 2010). The rise post-impact is due to heating of the inlet, embedded in the surface material.

immediately affected by evolved vapors. However, the overall timeline is probably representative – e.g. Fig. 11 shows the warming of the interior of the Top Hat, and the corresponding dew point of the ethane partial pressure measured by GCMS.

The saturation vapor pressure of pure ethane is very small (equivalent to a mixing ratio of about 30 ppm at Titan's surface temperature of 94 K) but rises steeply with temperature. Should surface material damp with ethane have warmed to 120–140 K, the saturation mixing ratio would increase to 0.2–2%. The GCMS data show that several other compounds rose in detected abundance over an hour or so after landing. Benzene and cyanogen were detected, and so it seems likely that a rich cocktail of hydrocarbons and nitriles (and, indeed, CO_2 , a well-known acoustic absorber) may have similarly accumulated in the Top Hat cavity.

Leese et al. (2012) noted that during API-V specific to experiment test on the flight model probe, which involved using a purpose built Top Hat non-flight cover to introduce several different gases and flush through the Top Hat cavity for each, carbon dioxide produced timeouts (i.e. no signal detected) for very low concentrations in nitrogen due to high acoustic absorption. In addition to this well-known effect of the pure gas, Garry (1996) noted in ground tests of the API-V system that an order of magnitude drop in signal was encountered when purging a test cavity with nitrogen after making measurements in ethane or methane. This transient attenuation due to nitrogen/methane or

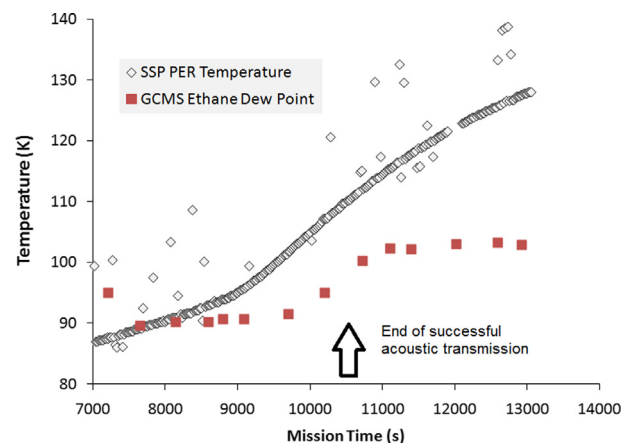


Fig. 11. Temperature evolution of the permittivity sensor near the front of the Top Hat: see e.g. Lorenz (2007). Although formally unrelated, the dew point of the ethane partial pressure indicated by the GCMS is also shown, illustrating the broad consistency between the rise of probe-base temperatures and the presence of volatiles. The period in which the pulse transit efficiency declines to zero is indicated, and corresponds with the rise in volatile abundance.

nitrogen/ethane mixtures could not be characterized in detail, unfortunately, since no means were available to measure the changing composition. Thus we call attention to the need for quantitative acoustic absorption measurements of nitrogen mixtures with other gases, at temperatures of around 100 K.

The statistical behavior of the lost pulses is interesting, in that bursts of pulses appear to break through above the detection threshold – e.g. at 9800–9900 s, these bursts are 5–10 s long, whereas later, at 10,000 s (see Fig. 12) the bursts are more like 20 s. Furthermore, when propagation is successful in one direction (e.g. T1) it is often also successful in the other, suggesting a common factor. One possibility might be that the gas supply and/or removal is discretized somehow, e.g. bubbles of gas released from the subsurface like a plopping mudpot. There is unfortunately little data to constrain such speculation, although any subsurface phenomena were evidently too weak to cause any disturbance measurable by the sensitive accelerometers and tiltmeters on the probe.

5. Conclusions

The speed-of-sound instrument, whose principal intended role on the payload was to measure the properties of Titan's seas, nonetheless provided some information during descent and after landing, and suggests that sound propagation was suppressed about 20 min after touchdown.

Clearly, using the function of a threshold detector in this way is not an ideal attenuation measurement, having a very modest dynamic range. Nonetheless, the most plausible interpretation of the cessation of signals post-landing is the evolution of absorbing vapors from the surface. This independent detection of volatiles reinforces the notion that the surface materials at the landing site were 'damp', and underscores that unexpected results can be obtained from acoustic instrumentation. We may recall the words of Charlotte Brontë: "Silence is of different kinds, and breathes different meanings."

One lesson is that the interpretation of a notionally-simple instrument in an unknown environment was rather complex. A housekeeping measurement of signal strength, even on a small subset of the measurements, would have greatly assisted interpretation. More ambitiously, the ability to measure at a range of frequencies – to conduct acoustic absorption spectroscopy – might permit identification of the absorbing gases. Of course on future Titan missions any such augmented capabilities would be in

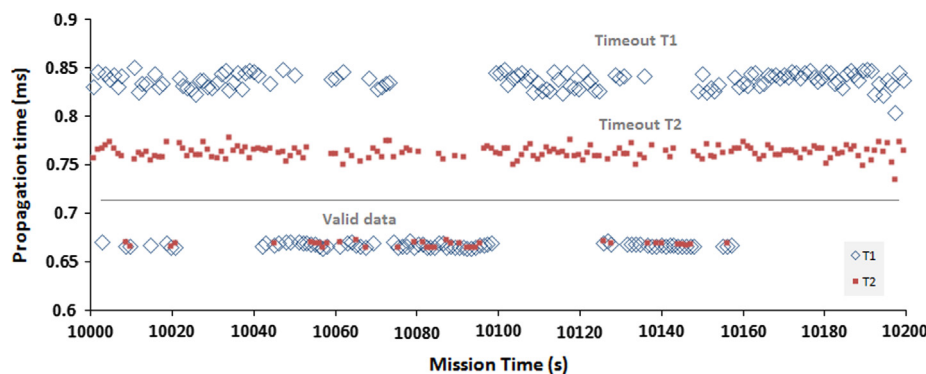


Fig. 12. Time series of data (essentially a zoom of Fig. 4) as the overall propagation probability was declining on the surface. Valid data tends to appear in bursts in both directions, here around 20 s long, with T2 tending to fail more often.

competition with a range of other scientific experiments and so the richness and significance of findings that might result must be traded off against the resource requirements and the opportunity costs of other types of instrumentation.

Acknowledgments

Cassini-Huygens is a joint endeavor of NASA, ESA and ASI. The results reported here were made possible by the efforts of many colleagues on the Huygens team. RL acknowledges the support of the Cassini project at the Jet Propulsion Laboratory, via NASA Grant NNX13AH14G. The lead author acknowledges useful discussions on acoustics with Juan Arvelo of APL and Tim Leighton of the University of Southampton. We thank Jean-Pierre Williams and an anonymous referee for helpful comments.

References

- Arvelo, J., Lorenz, R.D., 2013. Plumbing the depths of Ligeia: considerations for acoustic depth sounding in Titan's hydrocarbon seas. *J. Acoust. Soc. Am.* 134, 4335–4351.
- Bettanini, C., Zaccariotto, M., Angrilli, F., 2008. Analysis of the HASI accelerometers data measured during the impact phase of the Huygens probe on the surface of Titan by means of a simulation with a finite element model. *Planet. Space Sci.* 56, 715–727.
- Dain, Y., Lueptow, R.M., 2001. Acoustic attenuation in a three-gas mixture: results. *J. Acoust. Soc. Am.* 110, 2974–2979.
- Ejakov, S.G., Phillips, S., Dain, Y., Lueptow, R.M., Visser, J., 2003. Acoustic attenuation in gas mixtures with nitrogen: Experimental data and calculations. *J. Acoust. Soc. Am.* 113, 1871–1879.
- ESA, 2009. TSSM In-Situ Elements. Assessment Study Report, ESA-SRE(2008)4. European Space Agency, 12 February.
- Garry, J.R.C., 1996. Surveying Titan Acoustically (M.Sc. thesis). University of Kent at Canterbury, Canterbury (Garry, J.R.C., Kent, M.Sc., 1996, C3 46-9855).
- Hagermann, A., Rosenberg, P.D., Towner, M.C., Garry, J.R.C., Svedhem, H., Leese, M.R., Hathi, B., Lorenz, R.D., Zarnecki, J.C., 2007. Speed of sound measurements and the methane abundance in Titan's atmosphere. *Icarus* 189, 538–543.
- Hanford, A.D., Long, L.N., 2009. The direct simulation of acoustics on Earth, Mars and Titan. *J. Acoust. Soc. Am.* 125, 640–650.
- Holmes, R., Jones, G.R., Pusat, N., 1964. Vibrational relaxation in propane, propylene and ethane. *J. Chem. Phys.* 41, 2512–2516.
- JPL, 2010. Planetary Science Decadal Survey JPL Team X Titan Lake Probe Study. Final Report, Jet Propulsion Laboratory, April.
- Karkoschka, E., Tomasko, M.G., Doose, L.R., See, C., McFarlane, E.A., Schroeder, S.E., Rizk, B., 2007. DISR imaging and the geometry of the descent of Huygens. *Planet. Space Sci.* 55, 1896–1935.
- Karkoschka, E., Tomasko, M.G., 2009. Rain and dewdrops on titan based on in situ imaging. *Icarus* 199, 442–448.
- Leary, J., Jones, C., Lorenz, R., Strain, R.D. and Waite, J.H. 2007. Titan Explorer NASA Flagship Mission Study. JHU Applied Physics Laboratory, August 2007 (public release version January 2009). (http://www.lpi.usra.edu/opag/Titan_Explorer_Public_Report.pdf).
- Leese, M.R., Lorenz, R.D., Hathi, B., Zarnecki, J.C., 2012. The Huygens surface science package (SSP): flight performance review and lessons learned. *Planet. Space Sci.* 70, 28–45.
- Leighton, T.G., White, P.R., 2004. The sound of Titan – a role for acoustics in space exploration. *Acoust. Bull.* 29, 16–23.
- Leighton, T.G., Petculescu, A., 2009. The sound of music and voices in space. *Acoust. Today* 5, 17–29.
- Lorenz, R.D., 1994. Exploring the Surface of Titan (Ph.D. thesis). University of Kent at Canterbury.
- Lorenz, R.D., 2006. Thermal Interaction of the Huygens probe with the Titan environment: surface windspeed constraint. *Icarus* 182, 559–566.
- Lorenz, R.D., Niemann, H., Harpold, D., Zarnecki, J., Ground, Titan's Damp, 2006. Constraints on Titan surface thermal properties from the temperature evolution of the huygens GCMS inlet. *Meteorit. Planet. Sci.* 41, 1405–1414.
- Lorenz, R.D., Zarnecki, J.C., Towner, M.C., Leese, M.R., Ball, A.J., Hathi, B., Hagermann, A., Ghafoor, N.A.L., 2007. Descent motions of the Huygens probe as measured by the surface science package (SSP): turbulent evidence for a cloud layer. *Planet. Space Sci.* 55, 1936–1948.
- Lorenz, R.D., 2007. Titan atmosphere profiles from Huygens engineering (temperature and acceleration) sensors. *Planet. Space Sci.* 55, 1949–1958.
- Lorenz, R.D., Stofan, E., Junine, J.L., Zarnecki, J.C., Harri, A.-M., Karkoschka, E., Newman, C.E., Bierhaus, E.B., Clark, B.C., Yelland, M., Leese, M.R., Boldt, J., Darlington, E., Neish, C.D., Sotzen, K., Arvelo, J., Rasbach, C., Kretsch, W., Strohbehn, K., Grey, M., Mann, J., Zimmerman, H., Reed, C., 2012. MP3 – A meteorology and physical properties package for Titan air–sea studies. Abstract #1072 in International Workshop on Instrumentation for Planetary Missions, 1072.pdf, Goddard Space Flight Center, Lunar and Planetary Institute, October 2012.
- Martinsson, P.-E., Delsing, J., 2002. Ultrasonic measurements of molecular relaxation in ethane and carbon monoxide. In: *Proceedings of the 2002 IEEE Ultrasonics Symposium*, pp. 511–515.
- Niemann, H.B., Atreya, S.K., Bauer, S.J., Carignan, G.R., Demick, J.E., Frost, R.L., Gautier, D., Haberman, J.A., Harpold, D.N., Hunten, D.M., Israel, G., Lunine, J.L., Kasprzak, W.T., Owen, T.C., Paulkovich, M., Raulin, F., Raaen, E., Way, S.H., 2005. The abundances of constituents of Titan's atmosphere from the GCMS instrument on the Huygens probe. *Nature* 438, 779–784.
- Niemann, H.B., Atreya, S.K., Demick, J.E., Gautier, D., Haberman, J.A., Harpold, D.N., Kasprzak, W.T., Lunine, J.L., Owen, T.C., Raulin, F., 2010. Composition of Titan's lower atmosphere and simple surface volatiles as measured by the Cassini-Huygens probe gas chromatograph mass spectrometer experiment. *J. Geophys. Res.* 115, E12006, <http://dx.doi.org/10.1029/2010JE003659>.
- Pérez-Ayúcar, M., Lorenz, R.D., Flourey, N., Prieto, R., Lebreton, J.-P., 2006. Surface properties of Titan from post-landing reflections of the Huygens radio signal. *JGR – Planets* 111, E07001, <http://dx.doi.org/10.1029/2005JE002613>.
- Petculescu, A., Hall, B., Fraenzle, R., Phillips, S., Lueptow, R.M., 2006. A prototype acoustic gas sensor based on attenuation. *J. Acoust. Soc. Am.* 120, 1779–1782.
- Petculescu, A., Achi, P., 2012. A model for the vertical sound speed and absorption profiles in Titan's atmosphere based on Cassini-Huygens data. *J. Acoust. Soc. Am.* 131, 3671–3679.
- Petculescu, A., Lueptow, R.M., 2007. Atmospheric acoustics of Titan, Mars, Venus, and Earth. *Icarus* 186, 319–413.
- Rosenberg, P.D., 2007. Huygens' Measurements of the Speed of Sound on Titan (Ph. D. thesis). The Open University, Milton Keynes (A 2008 ETHOS/BL Reference number for the thesis is DXN116951).
- Schroeder, S.E., Karkoschka, E., Lorenz, R.D., 2012. Bouncing on Titan: motion of the Huygens probe in the seconds after landing. *Planet. Space Sci.* 73, 327–340.
- Stofan, E., Lorenz, R., Lunine, J., Bierhaus, E., Clark, B., Mahaffy, P., Ravine, M., 2013. TiME – The Titan Mare Explorer. In: *Proceedings of the IEEE Aerospace Conference*, Big Sky, MT, March, paper #2434.
- Svedhem, H., Lebreton, J.-P., Zarnecki, J.C., Hathi, B., 2004. Using speed of sound measurements to constrain the Huygens probe descent profile. *ESA SP 544*, 221–228.
- Towner, M.C., Garry, J.R.C., Lorenz, R.D., Hathi, B., Hagermann, A., Svedhem, H., Clark, B.C., Leese, M.R., Zarnecki, J.C., 2006. Physical properties of the Huygens landing site from the surface science package acoustic properties sensor (API S). *Icarus* 185, 457–465.
- Zarnecki, J.C., Banaszkiewicz, M., Bannister, M., Boynton, W.V., Challenor, P., Clark, B., Daniell, P.M., Delderfield, J., English, M.A., Garry, J.R.C., Geake, J.E., Green, S.F., Hathi, B., Jaroslowski, S., Leese, M.R., Lorenz, R.D., McDonnell, J.A.M., Merryweather-Clarke, N., Milli, C.S., Miller, R.J., Newton, G., Parker, D.J., Svedhem, H., Wright, M.J., 1997. The

- Huygens surface science package. In: Wilson, A. (Ed.), *Huygens: Science, Payload and Mission*. ESA SP-1177. ESA Publications Division, Noordwijk, pp. 177–195.
- Zarnecki, J.C., Leese, M.R., Garry, J.R.C., Ghafoor, N., Hathi, B., 2002. Huygens' surface science package. *Space Sci. Rev.* 104, 593–611.
- Zarnecki, J.C., Leese, M.R., Hathi, B., Ball, A.J., Hagermann, A., Towner, M.C., Lorenz, R.D., McDonnell, J.A.M., Green, S.F., Patel, M.R., Ringrose, T.J., Rosenberg, P.D., Atkinson, K. R., Paton, M.D., Banaszkiewicz, M., Clark, B.C., Ferri, F., Fulchignoni, M., Ghafoor, N.A. L., Kargl, G., Svedhem, H., Delderfield, J., Grande, M., Parker, D.J., Challenor, P.G., Geake, J.E., 2005. A soft solid surface on Titan at the Huygens landing site as measured by the surface science package (SSP). *Nature* 438 (7069), 792795.